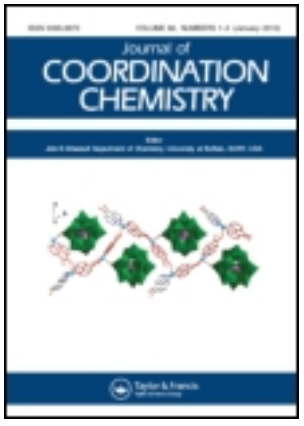

Journal of Coordination Chemistry
Publication details, including instructions for authors and subscription information:
http://www.tandfonline.com/loi/gcoo20

Syntheses, crystal structures, and fluorescent properties of 2-D Cd(II) complexes based on 2-(1H-imidazol-1-methyl)-1H-benzimidazole and 1,2,4,5-benzenetetracarboxylate ligands

Zhi-Wu Wang[a], Min Yu[a], Ting Li[a] & Xiang-Ru Meng[a]
[a] The College of Chemistry and Molecular Engineering, Zhengzhou University, Zhengzhou, PR China
Accepted author version posted online: 07 Nov 2013.Published online: 04 Dec 2013.

To cite this article: Zhi-Wu Wang, Min Yu, Ting Li & Xiang-Ru Meng (2013) Syntheses, crystal structures, and fluorescent properties of 2-D Cd(II) complexes based on 2-(1H-imidazol-1-methyl)-1H-benzimidazole and 1,2,4,5-benzenetetracarboxylate ligands, Journal of Coordination Chemistry, 66:23, 4163-4177, DOI: 10.1080/00958972.2013.861900

To link to this article: http://dx.doi.org/10.1080/00958972.2013.861900

Journal of Coordination Chemistry, 2013
Vol. 66, No. 23, 4163–4177, http://dx.doi.org/10.1080/00958972.2013.861900

Syntheses, crystal structures, and fluorescent properties of 2-D Cd(II) complexes based on 2-(1*H*-imidazol-1-methyl)-1*H*-benzimidazole and 1,2,4,5-benzenetetracarboxylate ligands

ZHI-WU WANG, MIN YU, TING LI and XIANG-RU MENG*

The College of Chemistry and Molecular Engineering, Zhengzhou University, Zhengzhou, PR China

(*Received 6 January 2013; accepted 10 October 2013*)

Two new complexes, $\{[Cd(btec)_{0.5}(imb)(CH_3OH)]\cdot CH_3OH\}_n$ (**1**) and $\{[Cd(btec)_{0.5}(H_2btec)]\cdot(H_2imb)\cdot 2H_2O\}_n$ (**2**) (H_4btec = 1,2,4,5-benzenetetracarboxylic acid, imb = 2-(1*H*-imidazol-1-methyl)-1*H*-benzimidazole), have been synthesized and characterized by elemental analysis and single-crystal X-ray diffraction. Both complexes exhibit 2-D network structures. In **1**, each 1,2,4,5-benzenetetracarboxylate links four Cd^{2+} cations, and each Cd^{2+} cation connects two 1,2,4,5-benzenetetracarboxylates, to form a 2-D layer, with the imb ligands located on each side of the 2-D layer. In **2**, there are two kinds of 1,2,4,5-benzenetetracarboxylates in the structure. One kind is completely deprotonated and acts as hexadentate linkers, leading to a 2-D layer. The other kind is only doubly deprotonated and decorates each side of the 2-D layer. In **2**, imb is protonated, forming $(H_2imb)^{2+}$ cations that only cocrystallize with the negatively charged Cd coordination polymer ($\{[Cd(btec)_{0.5}(H_2btec)]^{2-}\}_n$), but does not coordinate to the Cd^{2+} cations. IR spectra, PXRD patterns, thermogravimetric analyses, and fluorescent properties of **1** and **2** have also been determined.

Keywords: 2-(1*H*-imidazol-1-methyl)-1*H*-benzimidazole; 1,2,4,5-Benzenetetracarboxylate; Cadmium complex; Thermostability; Fluorescent property

1. Introduction

Over the past two decades, the crystal engineering of metal–organic frameworks (MOFs) has provoked unparalleled attention and imagination owing to their intriguing molecular topologies and potential applications in ion exchange, gas sorption and storage, catalysis, chemical sensing, drug delivery, optics, and magnetism [1]. However, it is still a challenge to predict the exact structures and compositions of assembly products, and further studies are required to understand the assembly process of metal salts and organic linkers. The results of our most recent studies showed that flexible multidentate ligands with *N*-heterocyclic groups, such as 2-(1*H*-imidazol-1-methyl)-1*H*-benzimidazole, 2-((1*H*-1,2,4-triazol-1-yl)methyl)-1*H*-benzimidazole, and 2-(1*H*-tetrazole-1methyl)-1*H*-benzimidazole, are excellent ligands for the construction of MOFs with specific structures and interesting properties, since these ligands have several potential *N*-donors and can act as both hydrogen bond acceptors and donors [2]. Aromatic polycarboxylic acid, especially 1,2,4,5-benzenetetracarboxylic acid

*Corresponding author. Email: mxr@zzu.edu.cn

(H_4btec), has been demonstrated to be a powerful ligand for MOF synthesis, since it possesses several interesting characteristics. One, it has four carboxylic acid groups, which may be partially or completely deprotonated, to coordinate to metal ions in a wide variety of coordination modes, allowing interesting structures with higher dimensionality. Two, it can act not only as a hydrogen-bond acceptor but also as a hydrogen-bond donor, depending upon the numbers of deprotonated carboxylate groups. Three, some of the carboxylate groups may not lie in the phenyl ring plane upon complexation to metal ions owing to steric hindrance, thus able to connect metal ions in different directions [3]. Employment of *N*-heterocyclic ligands and polycarboxylates is an effective approach for the construction of MOFs [4(a)]. For example, $\{[Cd_2(tttmb)_2(btec)(H_2O)_3]\cdot H_2O\}_n$ (tttmb = 1,3,5-tris-(triazol-1-ylmethyl)-2,4,6-(trimethylbenzene) reported by Hou *et al.* shows a 3-D topology with a Schläfli symbol of $(5^3)(5^2\cdot6^2\cdot7\cdot9)(5^5\cdot6^2\cdot7^2\cdot8)$ and can emit strong fluorescence in the visible region [4(a)]. Chen reported a series of Cd(Zn)-H_2L-polycarboxylate complexes (H_2L = 1-(1*H*-imidazol-4-yl)-3-(4*H*-tetrazol-5-yl)benzene, polycarboxylate = 5-methyl-1,3-benzenedicarboxylate, 1,2,4,5-benzenetetracarboxylate, 1,4-benzenedicarboxylate, 1,3-benzenedicarboxylate) with good photoluminescent properties [4(b)]. Considering the structural compatibility of mixed ligands in the construction of MOFs, our attention has been focused on reactions of various metal salts with flexible multidentate *N*-heterocyclic ligands and aromatic polycarboxylic acids with a number of complexes obtained [4(c)–(g)]. As a continuation of these efforts, we have carried out reactions of 2-(1*H*-imidazol-1-methyl)-1*H*-benzimidazole (imb) with 1,2,4,5-benzenetetracarboxylic acid (H_4btec) and $Cd(NO_3)_2\cdot3H_2O$. Herein, we report the syntheses, crystal structures, IR spectra, PXRD patterns, thermostability, and photoluminescent properties of two new complexes, $\{[Cd(btec)_{0.5}(imb)(CH_3OH)]\cdot CH_3OH\}_n$ (**1**) and $\{[Cd(btec)_{0.5}(H_2btec)]\cdot(H_2imb)\cdot2H_2O\}_n$ (**2**).

2. Experimental

2.1. *General information and materials*

2-(1*H*-imidazole-1-methyl)-1*H*-benzimidazole (imb) was synthesized according to the literature method [5]. All chemicals were of AR Grade from commercial sources and used without purification. The IR spectra of **1** and **2** were recorded as KBr pellets from 400–4000 cm^{-1} on a BRUKER TENSOR 27 spectrophotometer and a Nicolet NEXUS 470-FT-IR spectrophotometer, respectively. Elemental analyses were carried out on a FLASH EA 1112 elemental analyzer. Steady state fluorescence measurements were performed using a Hitachi F-4500 spectrofluorometer at room temperature in the solid state. PXRD patterns were recorded using Cu-Kα radiation on a PANalytical X'Pert PRO diffractometer. TG measurements were performed by heating the sample from 30–780 °C at 10 °C min^{-1} in air on a NETZSCH STA 409 PC/PG differential thermal analyzer.

2.2. *Synthesis of $\{[Cd(btec)_{0.5}(imb)(CH_3OH)]\cdot CH_3OH\}_n$ (1)*

An aqueous solution (5 mL) of $Cd(NO_3)_2\cdot4H_2O$ (0.1 mM) was added dropwise to a methanol solution (2 mL) of imb (0.1 mM). A DMF solution (1 mL) of H_4btec (0.2 mM) was then added dropwise into the above mixture, and the final reaction mixture was filtered to give a clear solution at room temperature. Colorless block-shaped crystals (21.4 mg, 43% yield based on Cd) suitable for X-ray analysis were obtained through slow crystallization in

a closed container after five weeks. Anal. Calcd for $C_{18}H_{19}CdN_4O_6$ (499.77) (%): C, 43.25; H, 3.83; N, 11.21. Found (%): C, 43.55; H, 3.91; N, 11.36. IR (KBr, cm^{-1}): 3472(m), 3132 (m), 1570(s), 1497(m), 1464(m), 1428(s), 1380(s), 1281(m), 1247(s), 1100(s), 1036(s), 937 (s), 874(s), 829(s), 810(s), 750(s), 656(s), 571(m), 534(m).

2.3. *Synthesis of {[Cd(btec)$_{0.5}$(H$_2$btec)]·(H$_2$imb)·2H$_2$O}$_n$ (2)*

A mixture of $Cd(NO_3)_2·4H_2O$ (0.1 mM), imb (0.1 mM), H_4btec (0.2 mM), DMF (1 mL), methanol (2 mL), and water (5 mL) was placed in a 25 mL Teflon-lined stainless steel vessel and heated at 80 °C for 72 h, then cooled to room temperature. Colorless block-shaped crystals (40.6 mg, 56% yield based on Cd) were collected, washed with distilled water, and dried in air. Anal. Calcd for $C_{26}H_{21}CdN_4O_{14}$ (725.87) (%): C, 43.02; H, 2.91; N, 7.72. Found (%): C, 43.13; H, 2.78; N, 7.98. IR (KBr, cm^{-1}): 3446(s), 3129(s), 2974(w), 1724 (s), 1682(s), 1572(s), 1492(m), 1439(s), 1418(s), 1366(s), 1269(m), 1257(m), 1117(s), 939 (m), 841(s), 819(s), 762(s), 622(s), 529(m).

2.4. *Single-crystal structure determination*

A suitable single crystal of **1** or **2** was carefully selected and glued to a thin glass fiber. Crystal structure determination by X-ray diffraction was performed on a Rigaku Saturn 724 CCD area detector with a graphite monochromator for the X-ray source (Mo Kα radiation, $\lambda = 0.71073$ Å) operating at 50 kV and 40 mA. The data were collected by ω scan mode at 293(2) K. An empirical absorption correction was applied. The data were corrected for Lorentz-polarization effects. The structures were solved by direct methods and refined by full-matrix least-squares and difference Fourier techniques, based on F^2, using SHELXS-97 [6]. All non-hydrogen atoms were refined anisotropically. Hydrogens bound to carbon and nitrogen in **1**, and hydrogens bound to carbon in **2** were placed in calculated positions. The hydrogen of the methanol hydroxyl group in **1** was found at reasonable positions in the difference Fourier map and refined. Hydrogens bound to nitrogen and hydrogens of water and non-deprotonated carboxylic acid of H_2btec^{2-} in **2** were located from the difference maps and refined. All hydrogens were included in the final refinement. Crystallographic and structural refinement parameters for **1** and **2** are summarized in table 1. Selected bond distances and angles are listed in table 2. Hydrogen bond parameters are listed in table 3.

3. Results and discussion

3.1. *IR spectroscopy of 1 and 2*

IR spectra show absorptions at 3472 cm^{-1} for **1** and 3446 cm^{-1} for **2**, which can be attributed to stretching vibrations of O–H. Absorptions at 3132 cm^{-1} for **1** and 3129 cm^{-1} for **2** originate from stretching vibrations of Ar–H. Separations (Δ) between υ_a(COO) and υ_s(COO) are different for unidentate, chelating, and bridging carboxylates [7]. In **1**, unidentate and chelating carboxylates are observed; the unidentate carboxylates exhibit υ_a(COO) and υ_s(COO) at 1570 and 1380 cm^{-1} (Δ = 190 cm^{-1}), whereas the chelating carboxylates exhibit υ_a(COO) and υ_s(COO) at 1497 and 1428 cm^{-1} (Δ = 69 cm^{-1}). In **2**, the coordination modes of the carboxylates are quite complicated. The υ_a(COO) and υ_s(COO) bands at 1492 and 1418 cm^{-1} (Δ = 74 cm^{-1}) can be assigned to stretching vibrations of chelating carboxylates. The υ_a(COO) and υ_s(COO) bands at 1572 and 1366 cm^{-1} (Δ = 206 cm^{-1}) can be

Table 1. Crystallographic and structural refinement parameters for **1** and **2**.

Complex	**1**	**2**
Empirical formula	$C_{18}H_{19}CdN_4O_6$	$C_{26}H_{21}CdN_4O_{14}$
Formula weight	499.77	725.87
Crystal system	Monoclinic	Monoclinic
Space group	$P2_1/c$	$P2_1/c$
Unit cell dimensions (Å, °)		
a	12.108(2)	19.426(4)
b	9.1862(18)	6.8439(14)
c	19.035(7)	19.537(4)
α	90	90
β	113.26(2)	103.13(3)
γ	90	90
Volume (Å^3), Z	1945.1(9), 4	2529.6(9), 4
Calculated density (Mg m^{-3})	1.707	1.906
Absorption coefficient (mm^{-1})	1.166	0.953
F (000)	1004	1460
R (int)	0.1019	0.0356
Data/restraints/parameters	3269/1/265	6006/2/376
Goodness-of-fit on F^2	1.120	1.108
Final R indices [$I > 2\sigma(I)$]	$R_1 = 0.0992$	$R_1 = 0.0346$
	$wR_2 = 0.2095$	$wR_2 = 0.0706$
R indices (all data)	$R_1 = 0.1201$	$R_1 = 0.0391$
	$wR_2 = 0.2238$	$wR_2 = 0.0732$

Table 2. Selected bond distances (Å) and angles (°) for **1** and **2**.

1			
Cd(1)−O(4)#1	2.243(10)	Cd(1)−N(4)	2.338(9)
Cd(1)−N(1)#2	2.338(10)	Cd(1)−O(1)	2.406(8)
Cd(1)−O(2)	2.442(9)	Cd(1)−O(5)	2.471(9)
O(4)#1−Cd(1)−N(4)	86.5(4)	O(4)#1−Cd(1)−N(1)#2	93.0(4)
N(4)−Cd(1)−N(1)#2	104.2(4)	O(4)#1−Cd(1)−O(1)	124.2(4)
N(4)−Cd(1)−O(1)	146.9(3)	N(1)#2−Cd(1)−O(1)	87.4(4)
O(4)#1−Cd(1)−O(2)	176.3(4)	N(4)−Cd(1)−O(2)	94.5(3)
N(1)#2−Cd(1)−O(2)	90.2(4)	O(1)−Cd(1)−O(2)	54.1(3)
O(4)#1−Cd(1)−O(5)	92.2(4)	N(4)−Cd(1)−O(5)	89.0(4)
N(1)#2−Cd(1)−O(5)	166.0(4)	O(1)−Cd(1)−O(5)	78.9(3)
O(2)−Cd(1)−O(5)	84.3(3)		
2			
Cd(1)–O(1)	2.3305(17)	Cd(1)–O(4)#1	2.3492(17)
Cd(1)–O(6)#1	2.3522(18)	Cd(1)–O(5)	2.3635(17)
Cd(1)–O(1)#1	2.3691(16)	Cd(1)–O(4)#2	2.3918(17)
Cd(1)–O(3)#2	2.4589(18)	Cd(1)–O(2)	2.735(2)
O(1)–Cd(1)–O(4)#1	79.84(6)	O(1)–Cd(1)–O(6)#1	98.54(6)
O(4)#1–Cd(1)–O(6)#1	77.16(6)	O(1)–Cd(1)–O(5)	93.19(6)
O(4)#1–Cd(1)–O(5)	84.43(6)	O(6)#1–Cd(1)–O(5)	155.97(6)
O(1)–Cd(1)–O(1)#1	157.39(5)	O(4)#1–Cd(1)–O(1)#1	78.61(6)
O(6)#1–Cd(1)–O(1)#1	83.25(6)	O(5)–Cd(1)–O(1)#1	78.03(6)
O(1)–Cd(1)–O(4)#2	123.60(6)	O(4)#1–Cd(1)–O(4)#2	156.55(5)
O(6)#1–Cd(1)–O(4)#2	96.65(6)	O(5)–Cd(1)–O(4)#2	94.15(6)
O(1)#1–Cd(1)–O(4)#2	78.21(6)	O(1)–Cd(1)–O(3)#2	78.78(6)
O(4)#1–Cd(1)–O(3)#2	141.00(6)	O(6)#1–Cd(1)–O(3)#2	74.28(6)
O(5)–Cd(1)–O(3)#2	128.88(6)	O(1)#1–Cd(1)–O(3)#2	122.94(6)
O(4)#2–Cd(1)–O(3)#2	54.14(6)	O(1)–Cd(1)–O(2)	51.15(5)
O(4)#1–Cd(1)–O(2)	120.02(6)	O(6)#1–Cd(1)–O(2)	134.40(6)
O(5)–Cd(1)–O(2)	68.62(6)	O(1)#1–Cd(1)–O(2)	138.70(6)
O(4)#2–Cd(1)–O(2)	80.58(6)	O(3)#2–Cd(1)–O(2)	67.42(6)

Note: Symmetry transformations used to generate equivalent atoms: For **1**: #1 $-x+2$, $y+1/2$, $-z+3/2$; #2 x, $y-1$, z. For **2**: #1 $-x+1$, $y-1/2$, $-z+1/2$; #2 x, $y-1$, z.

Table 3. Hydrogen bond parameters of **1** and **2**.

D−H···A	*d*(D−H) (Å)	*d*(H···A) (Å)	*d*(D···A) (Å)	(D−H···A) (°)
1				
O(5)−H(5)···O(1)#1	0.81	2.12	2.924(11)	172.3
N(3)−H(3B)···O(6)#6	0.86	1.98	2.797(16)	157.5
O(6)−H(6)···O(2)#7	0.82	2.27	2.989(17)	146.2
2				
O(12)–H(12)···O(14)#6	0.81(4)	1.89(4)	2.687(3)	168(4)
O(8)–H(8)···O(9)#7	0.81(4)	1.83(4)	2.631(3)	172(4)
O(14)–H(4W)···O(10)#8	0.86(4)	1.97(4)	2.833(4)	176(4)
N(2)–H(2)···O(10)#8	0.86(4)	1.82(4)	2.679(3)	170(4)
N(4)–H(4)···O(2)#8	0.82(4)	1.98(4)	2.777(3)	163(4)
O(14)–H(3W)···O(9)#5	0.74(4)	2.23(4)	2.968(4)	175(4)
O(13)–H(2W)···O(6)#1	0.84(4)	2.02(4)	2.850(3)	169(4)
O(13)–H(1W)···O(5)#3	0.80(4)	2.01(4)	2.802(3)	172(4)
N(1)–H(1)···O(13)	0.852(10)	1.904(19)	2.703(3)	155(4)

Note: Symmetry transformations used to generate equivalent atoms: For **1**: #1 $-x+2$, $y+1/2$, $-z+3/2$; #6 $-x+1$, $y+1/2$, $-z+3/2$; #7 x, $-y+3/2$, $z+1/2$. For **2**: #1 $-x+1$, $y-1/2$, $-z+1/2$; #3 $-x+1$, $y+1/2$, $-z+1/2$; #5 $-x+1$,$-y+1$,$-z+1$; #6 $x+1$, y, z; #7 x, $-y+1/2$, $z-1/2$; #8 $-x+1$, $-y$, $-z+1$.

attributed to the stretching vibrations of the bridging or asymmetrical, bidentate carboxylates. In addition, absorptions at 1724 and 1682 cm^{-1} are characteristic of nondeprotonated carboxylic acid groups remaining on H_2btec^{2-}.

3.2. *Crystal structure of {[Cd(btec)$_{0.5}$(imb)(CH$_3$OH)]·CH$_3$OH}$_n$ (1)*

Single-crystal X-ray diffraction analysis reveals that **1** crystallizes in the monoclinic space group $P2_1/c$. Its asymmetric unit contains one Cd^{2+}, one imb, one half of a $btec^{4-}$, one coordinated methanol, and an uncoordinated methanol. As shown in figure 1(a), each Cd^{2+} is coordinated by two nitrogens (N1#2, N4) from two imb and four oxygens (O1, O2, O4#1, and O5) from one chelating carboxylate (O1, O2), one monodentate carboxylate (O4#), and one coordinated methanol. The coordination environment of Cd(II) can be regarded as a distorted octahedron. The equatorial plane of the distorted octahedron is composed of O1, O2, O4#1, and N4, while the axial positions are occupied by O5 and N1#2 with a N1#2−Cd1−O5 bond angle of 166.0(4)°. Cd1 is approximately coplanar with the mean plane of the four equatorial atoms with a deviation of 0.0808 Å. The Cd−O bond distances are 2.243(10), 2.406(8), 2.442(9), and 2.480(9) Å and the Cd–N bond distances are 2.338(9) and 2.338(10) Å. These Cd−O/N distances are in the range of those observed in other Cd(II) complexes [8]. H_4btec is fully deprotonated, and the dihedral angles between the mean plane defined by the benzene ring and the chelating and monodentate coordinating carboxylate groups are 35.3° and 55.4°, respectively. Two *para*-carboxylates of the $btec^{4-}$ anion adopt bidentate chelating modes, chelating two Cd^{2+} cations, and the other two *para*-carboxylates are monodentate, connecting two Cd^{2+} cations (scheme 1, mode f). Hence each $btec^{4-}$ anion is a tetraconnector, linking four Cd^{2+} cations, and each Cd^{2+} connects two $btec^{4-}$ to form a 2-D layer structure that has rhombic windows with a side length of 9.280 Å and approximate diagonal measurement of 16.764×7.228 Å^2 (figure 1(b)). As illustrated in figure 1(c), each imb bridges two Cd^{2+} cations and the imb are located on each side of the 2-D layer. Furthermore, as shown in figure 1(d), there are three kinds of hydrogen bonds in **1**. Oxygen (O5) of coordinated methanol forms a hydrogen bond (O5···O1: 2.924(11) Å) with oxygen (O1) of a $btec^{4-}$ anion. Nitrogen (N3) of benzimidazole forms a hydrogen bond (N3···O6: 2.797(16) Å) with oxygen (O6) of uncoordinated methanol.

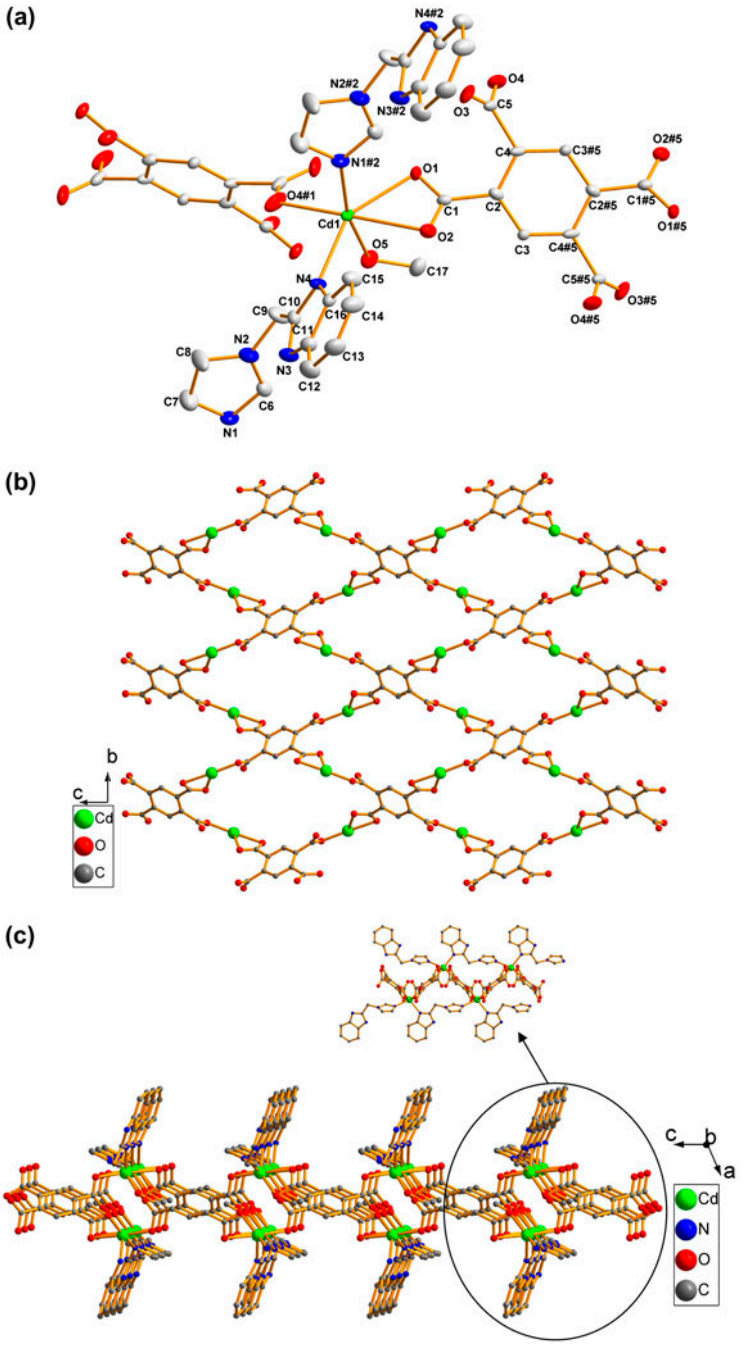

Figure 1. (a) Coordination environment of Cd(II) in **1** with atom numbering scheme and 30% probability ellipsoids. Uncoordinated methanol and hydrogens are omitted for clarity (#1 $-x+2$, $y+1/2$, $-z+3/2$; #2 x, $y-1$, z; #5 $-x+2$, $-y+1$, $-z+1$). (b) View of the 2-D structure of **1**; coordinated imb and methanol are omitted for clarity. (c) 2-D structure of **1** showing imb on each side of the 2-D layer. (d) View of hydrogen bonds in **1** (#1 $-x+2$, $y+1/2$, $-z+3/2$; #6 $-x+1$, $y+1/2$, $-z+3/2$; #7 x, $-y+3/2$, $z+1/2$). (e) 3-D structure of **1** linked through hydrogen bonds indicated by dashed lines (blue, O–H···O hydrogen bonds; green, N–H···O hydrogen bonds (see http://dx.doi.org/10.1080/00958972.2013.861900 for color version)).

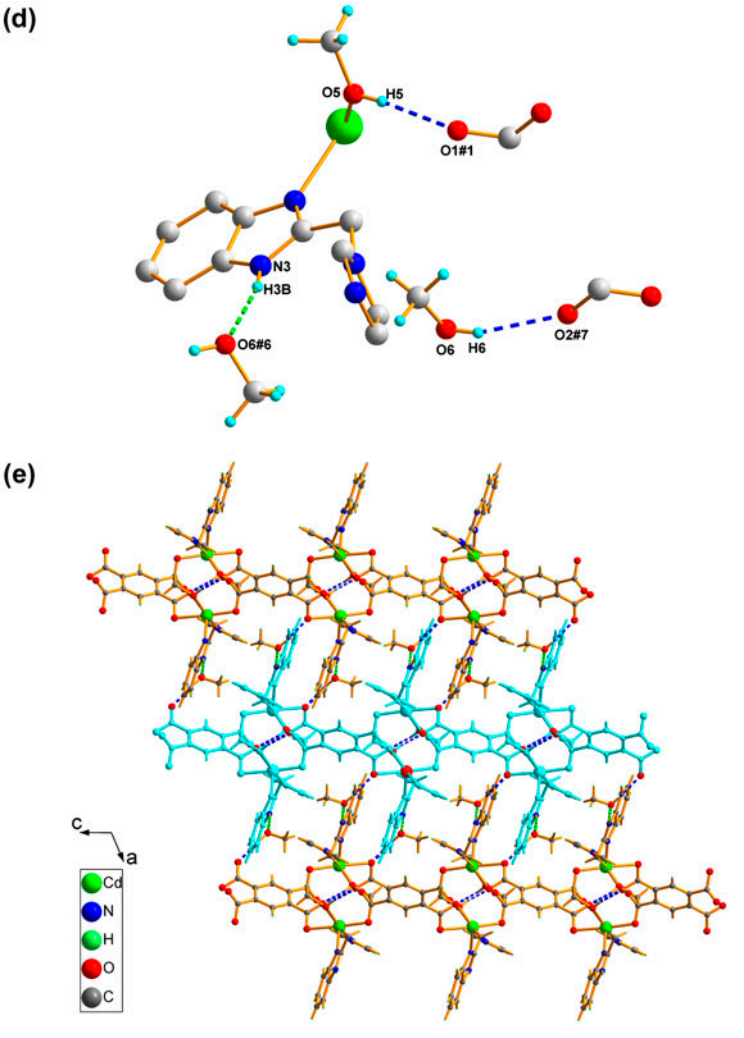

Figure 1. (*Continued*).

Oxygen (O6) of uncoordinated methanol forms another hydrogen bond (O6···O2: 2.989 (17) Å) with oxygen (O2) of the $btec^{4-}$ anion. N–H···O hydrogen bonds along with O–H···O hydrogen bonds link the 2-D layers and the uncoordinated methanol molecules into the 3-D structure (figure 1(e)).

3.3. *Crystal structure of* $\{[Cd(btec)_{0.5}(H_2btec)]\cdot(H_2imb)\cdot 2H_2O\}_n$ *(2)*

When the reaction temperature is increased from room temperature to 80 °C, **2** is isolated with a different structure than that of **1**. Imb is protonated forming a $(H_2imb)^{2+}$ cation that cocrystallizes with waters and the negatively charged Cd coordination polymer $\{[Cd(btec)_{0.5}(H_2btec)]^{2-}\}_n$, but does not coordinate to the Cd^{2+} cation. Single-crystal X-ray crystallography reveals that **2** features a 2-D network of $\{[Cd(btec)_{0.5}(H_2btec)]^{2-}\}_n$

sandwiched by $(H_2imb)^{2+}$ and waters. As depicted in figure 2(a), each Cd^{2+} anion is coordinated by seven oxygens (Cd1–O1: 2.3305(17), Cd1–O1#1: 2.3691(16), Cd1–O3#2: 2.4589(18), Cd1–O4#1: 2.3492(17), Cd1–O4#2: 2.3918(17), Cd1–O5: 2.3635(17), Cd1–O6#1: 2.3522(18) Å) from three $btec^{4-}$ anions and two H_2btec^{2-} anions. These bond distances are close to those observed in **1** and within the normal range [9]. Although the Cd1–O2 distance of 2.735(2) Å is somewhat longer than the other seven Cd1–O distances, it similar to Cd–O distances in complexes $[Cd_3(SIP)_2(bbi)_5{\cdot}3H_2O]_n$ (Cd-O: 2.713(3) and 2.753(3) Å, SI*p* = 5-sulfoisophthalate, bbi = 1,1′-(1,4-butanediyl)bis(imidazole), $[Cd_3(SIP)_2(bix)_4{\cdot}8\text{-}H_2O]_n$ (Cd–O: 2.725(2) Å, bix = 1,4-bis(imidazol-1-ylmethyl)-benzene) and $[Cd(HIDC)(bix)]_n$ (Cd–O: 2.7091(38) Å, H_3IDC = imidazole 4,5-dicarboxylic acid) [10, 11]. These suggest that there is a nonnegligible interaction between Cd1 and O2. Hence, the Cd^{2+} cation can also be regarded as eight-coordinate. Two types of H_4btec-derived anions, $btec^{4-}$ and H_2btec^{2-}, are present in the structure. For the completely deprotonated $btec^{4-}$ anion, the dihedral angles between the mean plane defined by the benzene ring and the planes of the carboxylates are 137.9° and 34.1°. Each carboxyl in $btec^{4-}$ is tridentate, connecting one Cd^{2+} cation in a chelating mode (O3#2, O4#2) and a second in a semi-chelating coordination mode (O1, O2). The third interaction is by two O atoms of adjacent carboxylate groups, O1#1 and O4#1, which share a common Cd(II) atom. Thus, each $btec^{4-}$ anion is a hexadentate metal linker connecting six Cd(II) atoms by 12 coordination bonds (scheme 1, mode o). The inter-connections of the Cd^{2+} ions by $btec^{4-}$ anions lead to a 2-D layer

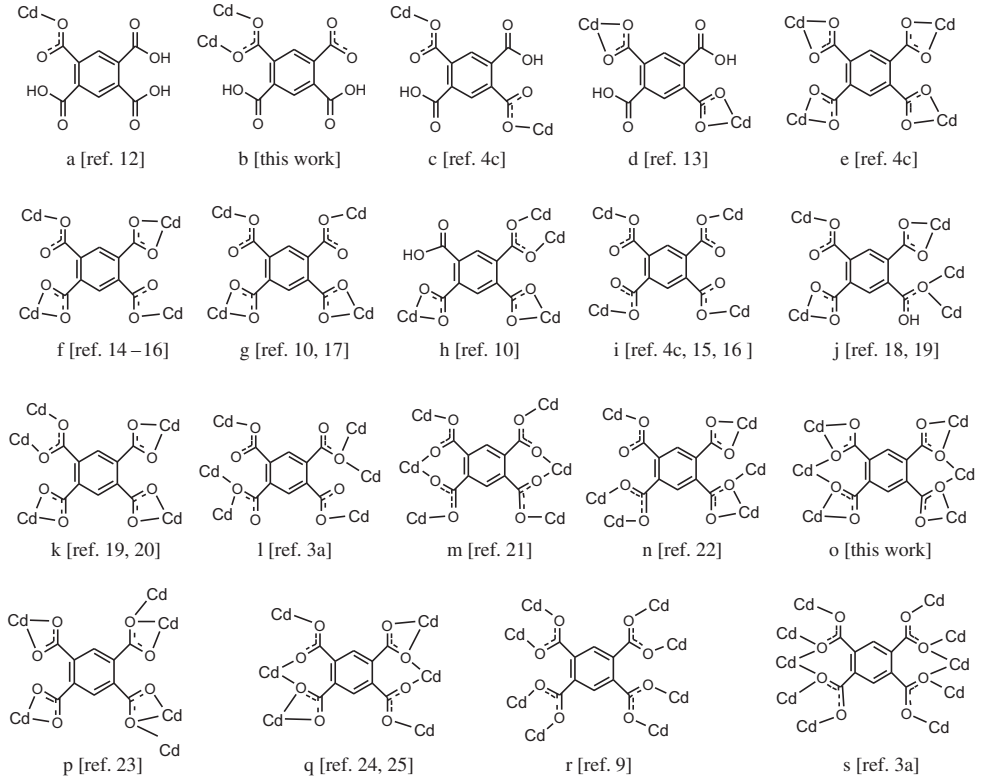

Scheme 1. Coordination modes of $btec^{4-}$ anions found in reported Cd–btec complexes (a, c–n, p–s) and the two new coordination modes in 2 (b, o).

parallel to the *bc* plane (figure 2(b)). The other anion, the doubly deprotonated H_2btec^{2-} anion, hangs at each side of the 2-D layer (figure 2(c)). Only one of the four carboxylate groups of H_2btec^{2-} is coordinated to a Cd^{2+} cation, that of the deprotonated carboxylate O5/O6, which has a bidentate bridging mode, connecting two Cd^{2+} cations (scheme 1, mode b). The dihedral angles between the mean plane defined by the benzene ring and the bridging carboxylate, uncoordinated carboxylate, and undeprotonated carboxylic acid groups are 98.1°, 92.2°, 12.3°, and 11.0°, respectively.

C–O bond distances in the deprotonated carboxylate groups are quite similar (C1–O1 = 1.275(3) Å, C1–O2 = 1.243(3) Å; C5–O3 = 1.242(3) Å, C5–O4 = 1.281(3) Å; C6–O5 = 1.257(3) Å, C6–O6 = 1.258(3) Å; C9–O9 = 1.252(3) Å, C9–O10 = 1.256(3) Å), and close to those in the related complexes $\{[Zn(Hbtc)(bmt)]\cdot DMF\cdot 5H_2O\}_n$ (1.274(4) and 1.233(4) Å, 1.238(4), and 1.274(4) Å; H_3btc = 1,3,5-benzenetricarboxylic acid, bmt = 2-((benzoimidazol-yl)methyl)1*H*-1,2,4-triazole), and $\{[Cd(Hbtc)(bmt)]\cdot 0.5DMF\cdot 0.5H_2O\}_n$ (1.241(5) and 1.227(5) Å, 1.238(5) and 1.242(5) Å) [2(d)]. But C–O bond distances in undeprotonated carboxylic acid groups are different (C7–O7 = 1.207(3) and C7–O8 = 1.324(3) Å; C8–O11 = 1.202(3), and C8–O12 = 1.317(3) Å), similar to those in reported complexes $\{[Zn(Hbtc)(bmt)]\cdot DMF\cdot 5H_2O\}_n$ (1.202(4) and 1.316(5) Å) and $\{[Cd(Hbtc)(bmt)]\cdot 0.5DMF\cdot 0.5H_2O\}_n$ (1.202(6) and 1.318(5) Å) [2(d)]. In addition, as shown in figure 2(d), there are three kinds N–H···O hydrogen bonds, between benzimidazole units and uncoordinated water, between benzimidazole units and carboxylates, between imidazole units and carboxylates, and six kinds of O–H···O hydrogen bonds, between carboxylic acid and carboxylates, between carboxylic acid groups and uncoordinated water, and between uncoordinated water and carboxylates. The 2-D layers, uncoordinated H_2imb^{2+} cations and uncoordinated water are further connected through the above nine kinds of hydrogen bonds forming the 3-D structure (figure 2(e)).

Through investigation of reported literature, 17 different coordination modes have been identified in Cd–btec complexes (scheme 1, modes a, c–n, p–s) [3(a), 4(c), 9, 10, 12–25]. Further study showed that the change of auxiliary ligands or reaction conditions can influence the coordination modes of the H_4btec-derived anions and the coordination environment of the Cd^{2+} cation and thus influence the structures of the complexes. For example, $[Cd_2(btec)(H_2O)]\cdot 0.8DMF$ was obtained from the $Cd(NO_3)_2$-H_4btec-DMF system at 130 °C, and it has a 3-D architecture with 1-D rhombic channels in which the $btec^{4-}$ anion coordinates to Cd^{2+} cation in mode n (scheme 1). The Cd^{2+} cations are six- and eight-coordinate [22]. $\{[Cd(btec)_{0.5}(H_2O)_3]\cdot H_2O\}_n$ was obtained from the $Cd(NO_3)_2$-H_4btec-MeOH-H_2O at 120 °C. It displayed an infinite 1-D chain structure in which a $btec^{4-}$ anion coordinates to a Cd^{2+} cation in mode f (scheme 1), and the Cd^{2+} cation is six-coordinate [26]. Through changing of the auxiliary ligands L, a series of Cd-btec-L complexes have been obtained, such as 3-D complex $[Cd_3(btec)(L)_2(H_2O)]\cdot H_2O$ (L = 5-(quinolyl)tetrazole) in which the $btec^{4-}$ anion coordinates to the Cd^{2+} cation in mode p (scheme 1) [23], 2-D complex $\{[Cd(btec)_{0.5}(L)H_2O]\cdot 4H_2O\}_n$ (L = 2-((1*H*-1,2,4-triazol-1-yl)methyl)-1*H*-benzimidazole) in which $btec^{4-}$ coordinates to the Cd^{2+} in mode e (scheme 1) [4(c)] and 1-D complex $[Cd_4(btec)_2(L)_4(H_2O)_4]_n$ (L = 1,10-phenanthroline) in which $btec^{4-}$ coordinates to the Cd^{2+} in modes f and i (scheme 1) [16]. In this work, by modifying the auxiliary ligand, two new 2-D Cd-btec-L complexes, **1** and **2**, were isolated in the presence of imb. The $btec^{4-}$ and H_2btec^{2-} anions display three coordination modes, of which the coordination in **2** are unprecedented (scheme 1, modes b, o). These results indicate that $btec^{4-}$ is a powerful ligand, and that the nature of auxiliary ligand plays significant roles in dominating molecular self-assembled structure.

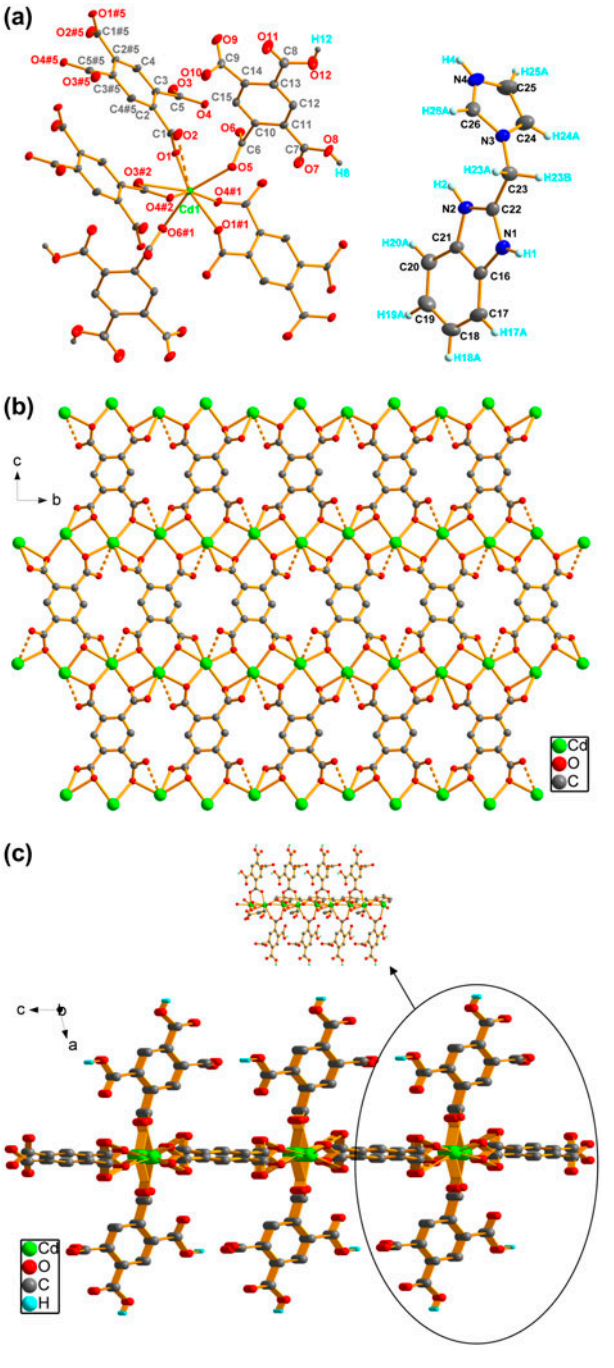

Figure 2. (a) Coordination environment of Cd(II) and $(H_2imb)^{2+}$ in **2** with atom numbering scheme and 50% probability ellipsoids. Uncoordinated water and hydrogens bound to carbons are omitted for clarity (#1 $-x+1$, $y-1/2$, $-z+1/2$; #2 x, $y-1$, z; #5 $-x+1$, $-y+1$, $-z+1$). (b) View of the 2-D structure of **2**; the $(H_2btec)^{2-}$ anions are omitted for clarity. (c) 2-D structure of **2** showing $(H_2btec)^{2-}$ anions on each side of the 2-D layer. (d) View of hydrogen bonds in **2** (#1 $-x+1$, $y-1/2$, $-z+1/2$; #3 $-x+1$, $y+1/2$, $-z+1/2$; #5 $-x+1$, $-y+1$, $-z+1$; #6 $x+1$, y, z; #7 x, $-y+1/2$, $z-1/2$; #8 $-x+1$, $-y$, $-z+1$). (e) 3-D structure of **2** linked through hydrogen bonds indicated by dashed lines (blue, O–H···O hydrogen bonds; green, N–H···O hydrogen bonds (see http://dx.doi.org/10.1080/00958972.2013.861900 for color version)).

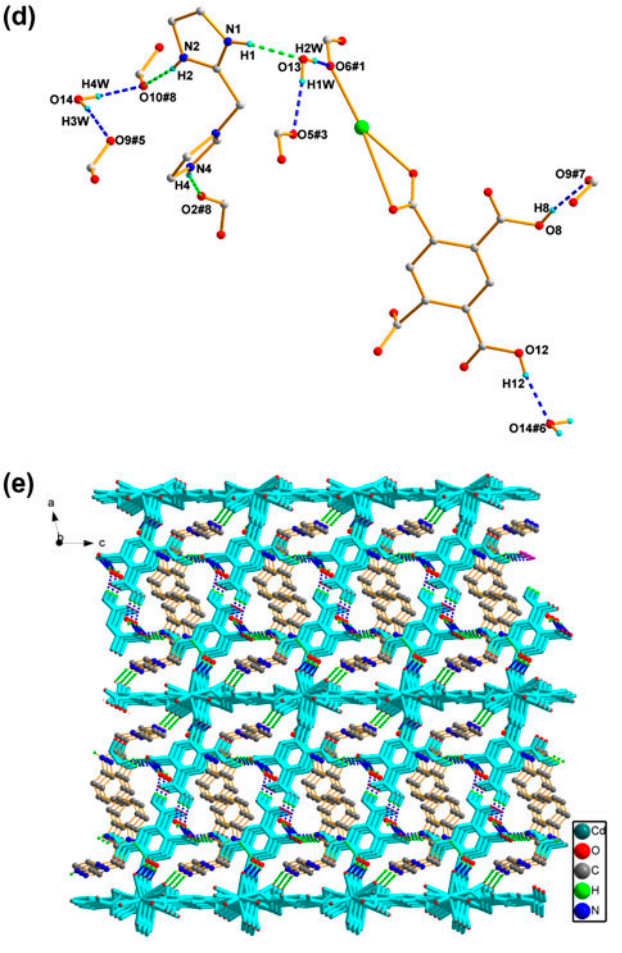

Figure 2. (*Continued*).

3.4. *PXRD Patterns and thermogravimetric analyses*

To confirm that the crystal structures are truly representative of the bulk materials, PXRD (powder X-ray diffraction) experiments were carried out for **1** and **2**. As shown in figure 3, the experimental PXRD patterns correspond well with the results simulated from the single-crystal data, indicating high purity of the synthesized samples, and single phases of both complexes are formed.

Thermogravimetric analyses of **1** and **2** were performed by heating the complexes from 30 to 780 °C in air. As shown in figure 4, the TG curve of **1** exhibits first mass loss of 12.56 wt.% between 38 and 148 °C, corresponding to release of solvent and coordination methanol (Calcd 12.82 wt.%). The solid then continues to lose mass from 297 to 668 °C, corresponding to decomposition of imb and $btec^{4-}$ anions. No further weight loss occurs up to 780 °C. The residue of 25.05 wt.% can be attributed to CdO (Calcd 25.69 wt.%). The TG curve of **2** reveals a weight loss of 5.12 wt.% from 59 to 123 °C, which can be assigned

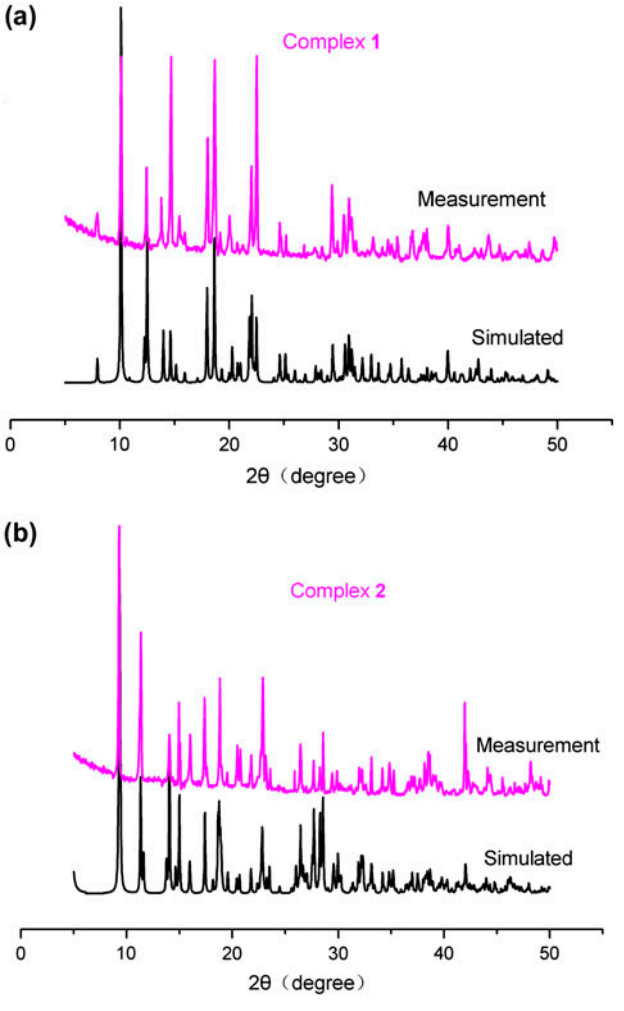

Figure 3. The PXRD patterns of **1** (a) and **2** (b) at room temperature; simulated patterns are generated from single-crystal diffraction data.

to the release of water (Calcd 4.97 wt.%). Continuous weight loss from 208 to 613 °C corresponds to decomposition of $(H_2imb)^{2+}$ and $btec^{4-}$ anions. No weight loss is observed from 613 to 780 °C. The residue of 17.14 wt.% is consistent with CdO (Calcd 17.69 wt.%). All these results are in agreement with the aforementioned crystal structures.

3.5. *Fluorescence*

A number of polynuclear d^{10} transition metal complexes, such as Zn(II) and Cd(II) complexes, exhibit interesting luminescence [11(b), 27]. Therefore, the solid-state emission spectra of **1** and **2** were investigated. As shown in figure 5, **1** exhibits luminescence with an emission maximum at 443 nm upon excitation at 338 nm and **2** displays luminescence with an emission maximum at 432 nm upon excitation at 334 nm. In order to understand the

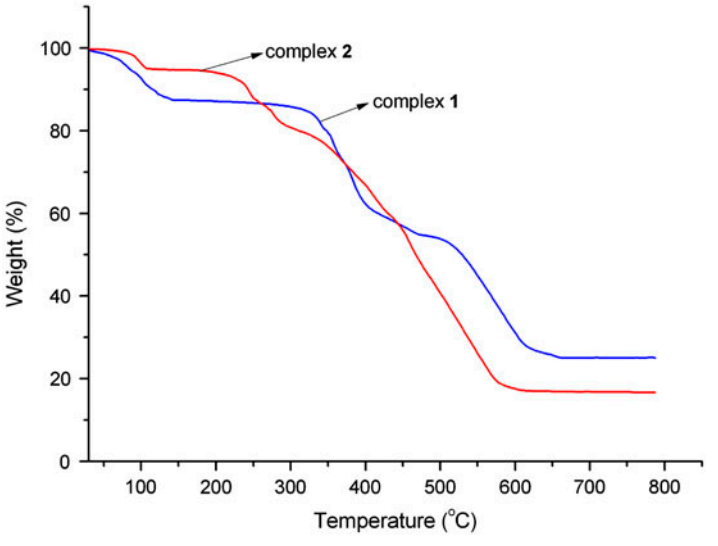

Figure 4. TG curves of **1** and **2**.

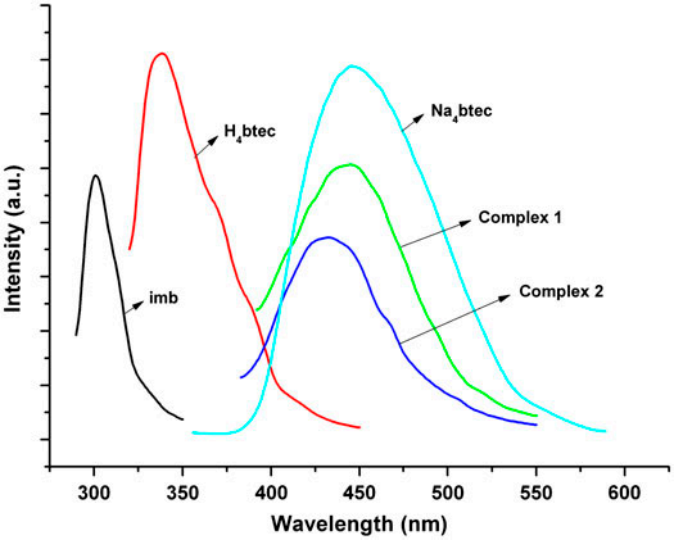

Figure 5. Solid-state emission spectra of free imb, H_4btec, Na_4btec, **1** and **2** at room temperature.

nature of the emission bands of **1** and **2**, the solid-state emission spectra of free imb, H_4btec, and Na_4btec were also recorded at room temperature. Free imb gives an emission band at 301 nm upon excitation at 285 nm, H_4btec shows an emission band with a maximum at 338 nm (λ_{ex} = 310 nm), and Na_4btec displays fluorescence with the maximum at 447 nm (λ_{ex} = 303 nm). Usually, fluorescence emissions from aromatic polycarboxylic acids

are different from the corresponding anions due to the different π-conjugated systems. Complexes **1**, **2**, and Na_4btec exhibit similar emission peaks, so the fluorescence emissions of **1** and **2** can mainly be assigned to intraligand transitions within the $btec^{4-}$ anion [4(e), 28].

4. Conclusion

Tetracarboxylate ligands like 1,2,4,5-benzenetetracarboxylate, biphenyl-3,3′,4,4′-tetracarboxylate, biphenyl-2,5,2′,5′-tetracarboxylate, and 2-(dimethylcarbamoyl)-biphenyl-5,2′,5′-tricarboxylate can adopt a variety of coordination modes in reactions with metal ions and may induce core aggregation, and thus should be feasible for linking discrete clusters into extended high-connected networks [3(a), 29]. In this article, through reaction of $Cd(NO_3)_2{\cdot}4H_2O$ with 1,2,4,5-benzenetetracarboxylic acid in the presence of 2-(1*H*-imidazole-1-methyl)-1*H*-benzimidazole, two new 2-D complexes, $\{[Cd(btec)_{0.5}(imb)(CH_3OH)]\cdot CH_3OH\}_n$ (**1**), and $\{[Cd(btec)_{0.5}(H_2btec)]\cdot(H_2imb)\cdot 2H_2O\}_n$ (**2**), have been synthesized. Their structures are different from reported Cd-btec complexes, and the 1,2,4,5-benzenetetracarboxylate anions in **2** display two new types of coordination (scheme 1, modes b and o). The results not only imply that 1,2,4,5-benzenetetracarboxylic acid possesses variable coordination modes in construction of MOFs, but they also show that distinct auxiliary ligands and reaction conditions play crucial roles in modulating the formation of the resulting coordination complexes. Combination of *N*-heterocyclic and polycarboxylate ligands is a good choice for construction of MOFs with specific structures and properties.

Supplementary material

Crystallographic data reported in this article have been deposited with the Cambridge Crystallographic Data Center as supplementary publication. CCDC numbers are 917545 and 917546. This data can be obtained free of charge via http://www.ccdc.cam.ac.uk/conts/retrieving.html (or from the Cambridge Crystallographic Data Center, 12 Union Road, Cambridge CB2 1EZ, UK; Fax: +44 1223 336 033).

Acknowledgment

We gratefully acknowledge the financial support by the National Natural Science Foundation of China (No. J1210060).

Supplemental data

Supplemental data for this article can be accessed http://dx.doi.org/10.1080/00958972.2013.861900.

References

[1] (a) K. Takaoka, M. Kawano, T. Hozumi, S. Ohkoshi, M. Fujita. *Inorg. Chem.*, **45**, 3976 (2006); (b) B.A. Blight, R. Guillet-Nicolas, F. Kleitz, R.Y. Wang, S. Wang. *Inorg. Chem.*, **52**, 1673 (2013); (c) M.P. Suh, H.J. Park, T.K. Prasad, D.W. Lim. *Chem. Rev.*, **112**, 782 (2012); (d) J.W. Shin, J.M. Bae, C. Kim, K.S. Min.

Inorg. Chem., **52**, 2265 (2013); (e) L.E. Kreno, K. Leong, O.K. Farha, M. Allendorf, R.P. Van Duyne, J.T. Hupp. *Chem. Rev*., **112**, 1105 (2012); (f) P. Horcajada, R. Gref, T. Baati, P.K. Allen, G. Maurin, P. Couvreur, G. Ferey, R.E. Morris, C. Serre. *Chem. Rev*., **112**, 1232 (2012); (g) Y. Gong, P.G. Jiang, J. Li, T. Wu, J.H. Lin. *Cryst. Growth Des*., **13**, 1059 (2013); (h) M. Wriedt, A.A. Yakovenko, G.J. Halder, A.V. Prosvirin, K.R. Dunbar, H.C. Zhou. *J. Am. Chem. Soc*., **135**, 4040 (2013); (i) K.P. Rao, M. Higuchi, J. Duan, S. Kitagawa. *Cryst. Growth Des*., **13**, 981 (2013).

[2] (a) T. Li, X. Su, Y. Xiu, X.R. Meng. *J. Coord. Chem*., **65**, 1792 (2012); (b) X. Su, T. Li, Y. Xiu, X.R. Meng. *Z. Naturforsch*., **67b**, 678 (2012); (c) S.X. Yan, G.H. Jin, Y. Yang, X. Su, X.R. Meng. *Synth. React. Inorg. Met.-Org. Chem*., **42**, 678 (2012); (d) B.T. Liu, R. Wang, G.H. Jin, X.R. Meng. *J. Coord. Chem*., **66**, 1784 (2013); (e) G.H. Jin, Y. Yang, X.L. Zhou, X.R. Meng. *Z. Naturforsch*., **67b**, 29 (2012); (f) G.H. Jin, R. Wang, Y. Xiu, Y. Yang, X.R. Meng. *Synth. React. Inorg. Met.-Org. Chem*., **42**, 596 (2012); (g) X.R. Meng, X.J. Wu, D.W. Li, H.W. Hou, Y.T. Fan. *Polyhedron*, **29**, 2619 (2010); (h) J. Zhang, B.D. Li, X.J. Wu, H.X. Yang, W. Zhou, X.R. Meng, H.W. Hou. *J. Mol. Struct*., **984**, 276 (2010); (i) Y.N. Ding, X.L. Zhou, G.H. Jin, D. Zhao, X.R. Meng. *Synth. React. Inorg. Met.-Org. Chem*., **42**, 438 (2012).

[3] (a) Y.Q. Sun, J. Zhang, G.Y. Yang. *J. Coord. Chem*., **57**, 1299 (2004); (b) Y.T. Ren, Y.X. Zhi, J. Hu, Y.Q. Zheng. *Synth. React. Inorg. Met.-Org. Chem*., **40**, 65 (2010); (c) L.J. Gao, P.X. Cao, J.J. Wang, Y.P. Wu, F. Fu, M.L. Zhang, Y.X. Ren, X.Y. Hou. *J. Coord. Chem*., **64**, 1299 (2011); (d) X.H. Li, Y.P. Wang, Z.Y. Ma, R.L. Zhang, J.S. Zhao. *J. Coord. Chem*., **63**, 1029 (2010).

[4] (a) X.J. Wang, Y.H. Liu, C.Y. Xu, Q.Q. Guo, H.W. Hou, Y.T. Fan. *Cryst. Growth Des*., **12**, 2435 (2012); (b) S.S. Chen, R. Qiao, L.Q. Sheng, Y. Zhao, S. Yang, M.M. Chen, Z D. Liu, D.H. Wang. *CrystEngComm*, **15**, 5713 (2013); (c) X. Han, X.X. Wang, G.H. Jin, X.R. Meng. *J. Coord. Chem*., **66**, 800 (2013); (d) S.X. Yan, D. Zhao, T. Li, R. Wang, X.R. Meng. *J. Coord. Chem*., **65**, 945 (2012); (e) D. Zhao, Y. Xiu, X.L. Zhou, X.R. Meng. *J. Coord. Chem*., **65**, 112 (2012); (f) B.T. Liu, D. Zhao, T. Li, X.R. Meng. *J. Coord. Chem*., **66**, 139 (2013); (g) X.X. Wang, X. Han, Z. Qiao, G.H. Jin, X.R. Meng. *Z. Naturforsch*., **67b**, 783 (2012).

[5] A.R. Katritzky, M. Drewniak-Deyrup, X.F. Lan. *Heterocycl. Chem.*, **26**, 829 (1989).

[6] G.M. Sheldrick. *Acta Cryst.*, **A64**, 112 (2008).

[7] K. Nakamoto. *Infrared and Raman Spectra of Inorganic and Coordination Compounds*. Part B, 6th Edn, p. 64, John Wiley, Hoboken, NJ (2009).

[8] R.H. Cui, Y.H. Xu, Z.H. Jiang. *Inorg. Chem. Commun.*, **12**, 933 (2009).

[9] H.Y. Bai, J.F. Ma, J. Yang, Y.Y. Liu, H. Wu, J.C. Ma. *Cryst. Growth Des.*, **10**, 995 (2010).

[10] J.D. Lin, J.W. Cheng, S W. Du. *Cryst. Growth Des.*, **8**, 3345 (2008).

[11] (a) L.L. Wen, Z.D. Lu, J.G. Lin, Z.F. Tian, H.Z. Zhu, Q.J. Meng. *Cryst. Growth Des*., **7**, 93 (2007); (b) L.L. Wen, Y.Z. Li, Z.D. Lu, C.Y. Duan, Q.J. Meng. *Cryst. Growth Des*., **6**, 530 (2006).

[12] L. Zhao, B.T. Liu, G.H. Jin, X.R. Meng. *Acta Cryst.*, **E68**, m139 (2012).

[13] Y.Y. Liu, J. Liu, J. Yang, B. Liu, J.F. Ma. *Inorg. Chim. Acta*, **403**, 85 (2013).

[14] J.F. Song, R.S. Zhou, X.Y. Xu, Y.B. Liu, T.G. Wang, J.Q. Xu. *J. Mol. Struct.*, **874**, 34 (2008).

[15] X. Shi, G.S. Zhu, X.H. Wang, G.H. Li, Q.R. Fang, G. Wu, G. Tian, M. Xue, X.J. Zhao, R.W. Wang, S.L. Qiu. *Cryst. Growth Des.*, **5**, 207 (2005).

[16] Q. Shi, R. Cao, D.F. Sun, M.C. Hong, Y.C. Liang. *Polyhedron*, **20**, 3287 (2001).

[17] R. Prajapati, L. Mishra, K. Kimura, P. Raghavaiah. *Polyhedron*, **28**, 600 (2009).

[18] X.J. Gu, Y.H. Chen, J. Peng, Z.Y. Shi, E.B. Wang, N.H. Hu. *J. Mol. Struct.*, **697**, 231 (2004).

[19] Y.Y. Jia, X.N. Xie, H.X. Yang. *Acta Cryst.*, **E68**, m801 (2012).

[20] L.Y. Wang, Y. Yang, K. Liu, B.L. Li, Y. Zhang. *Cryst. Growth Des.*, **8**, 3902 (2008).

[21] J.Y. Wu, C.H. Chang, T.W. Tseng, K.L. Lu. *J. Mol. Struct.*, **796**, 69 (2006).

[22] C.Y. Gao, S.X. Liu, L.H. Xie, Y.H. Ren, R.G. Cao, J.F. Cao, X.Y. Zhao. *J. Mol. Struct.*, **891**, 384 (2008).

[23] L. Ma, N.Q. Yu, S.S. Chen, H. Deng. *CrystEngComm*, **15**, 1352 (2013).

[24] Q. Hua, Y. Zhao, G.C. Xu, M.S. Chen, Z. Su, K. Cai, W.Y. Sun. *Cryst. Growth Des.*, **10**, 2553 (2010).

[25] Z.L. Xie, M.T. Feng, J.R. Li, X.Y. Huang. *Inorg. Chem. Commun.*, **11**, 1143 (2008).

[26] X. Han, X.X. Wang, Y. Yang, X.R. Meng. *Synth. React. Inorg. Met.-Org. Chem.*, **44**, 203 (2014).

[27] J. Tao, X. Yin, Z.B. Wei, R.B. Huang, L.S. Zheng. *Eur. J. Inorg. Chem.*, **2004**, 125, (2004).

[28] P.K. Chen, Y.X. Che, Y.M. Li, J.M. Zheng. *J. Solid State Chem.*, **179**, 2656 (2006).

[29] (a) R.H. Cui, G.J. Xu, Z.H. Jiang. *J. Coord. Chem*, **64**, 222 (2011); (b) S.Q. Guo, D. Tian, Y.H. Luo, H. Zhang. *J. Coord. Chem*., **65**, 308 (2012).